20th Australasian Fluid Mechanics Conference
Perth, Australia
5-8 December 2016

Experimental Investigation of a Regenerative Combustion Chamber for Ultra Micro Gas Turbines

V. Giovannoni[1], R.N. Sharma[1] and R.R. Raine[1]

[1]Department of Mechanical Engineering
The University of Auckland, Auckland 1142, New Zealand

Abstract

The ongoing development of small scale portable devices such as electronic systems, Global Positioning Systems (GPS), Unmanned Aerial Vehicles (UAV), exoskeletons for military applications and drones require power supplies with small dimensions and high energy density. The Ultra Micro Gas Turbine (UMGT) is a suitable candidate to fulfil these requirements, however there are only a few existing prototypes since downscaling from a conventional scale gas turbine system introduces many challenges. One of the major issues is the great amount of heat lost from the hot components to the surroundings which poses a limit to the overall thermal efficiency. This can be improved by recovering the heat lost from the combustion products to increase the temperature of the reactants mixture before combustion, yielding at the same time benefits in terms of flammability limits and pollutant emissions. For this purpose, a flat flame regenerative combustion chamber including a sintered steel porous medium as flame holder has been developed and tested. The regeneration occurs in two separate channels surrounding the combustion chamber, where cold reactants and exhaust gases flow respectively. Tests are run varying the mixture flow rate and the equivalence ratio and measuring emissions and temperature at different points within the combustor. Results for heat release rates (HRR) between 65 W and 565 W show that clean combustion of LPG is achieved with combustion efficiency higher than 99% for lean mixtures. Reactants' temperatures can reach values of up to around 900 K before entering the combustion chamber, showing a good level of regeneration.

Introduction

The development of small scale power systems as Ultra-Micro Gas Turbines (UMGT) began with the increasing demand for portable and compact power sources with high energy density able to replace current battery packages, which are heavy and require long recharge times [1-3]. With the development of new manufacturing techniques this option has become more feasible as the downscaling of components has reached sub-millimeter sizes. However there are still many challenges to be solved such as the low overall efficiency due to the great amount of heat losses, developing materials able to withstand combined high temperatures (≈1600 K) and mechanical stress, developing high rotational speed bearings and fluid dynamic losses due to clearance between static and rotating components [4-6].

The first approach towards UMGT dates back to the mid-1990s at MIT [3] where a device made up of six silicon wafers with dimensions 21×21×3.7 mm, able to generate a shaft power of 17 W when fuelled with hydrogen, was developed and tested. It was concluded that the thermal management had to be improved, high speed bearings needed to be developed, stronger materials had to be investigated and tip clearance had to be accurately studied to avoid fluid dynamic losses.

Since the first attempt at the MIT, a number of other groups have considered the development of the UMGT and its components over the years. These include the flat flame combustor at Tokyo Metropolitan University [2], the UMGT for the PowerMEMS project [7], the axial turbine at K.U. Leuven [8] and the project at ONERA [9] where a 10 mm diameter compressor was coupled with a radial turbine and a can type combustor. This last device was able to produce 50 W of electric power with a rotational speed of around 840,000 rpm. In 2012 IHI Corp. [10] announced the development of a 400 W UMGT incorporated in a portable suitcase. It is designed to be fuelled with propane, the turbine is 80 mm in diameter and it is able to reach a rotational speed of 400,000 rpm. Recently at the University of Auckland experiments on the effects of preheating the fuel/air mixture in a flat flame combustor with diameter of 46 mm have been carried out, achieving clean combustion and proving the beneficial effects on the flammability limits of natural gas [11].

The present work shows the results of the tests on a regenerative combustion chamber utilizing LPG, in terms of the level of reactant preheating that is achieved, emissions and thermal performance over a range of equivalence ratios and reactant mass flow rates.

Experimental apparatus

The section of the regenerative combustion chamber under investigation is shown in Figure 1. It is made up of two concentric cylinders where spiralling fins have been machined on the outer surfaces and an external wall. The stainless steel parts are then pressed together to keep them in place. A sintered steel porous medium (provided by Siperm Tridelta Gmbh) with 10 mm thickness, porosity in the range 0.49-0.54 and average pore size of 200 µm is placed in the combustion chamber to achieve flat flame on its surface and to allow optimal mixing of the reactants. The combustor is sealed on the upper and lower faces by two stainless steel plates kept together by bolts. The recirculation of the combustion products occurs in a cavity in the bottom plate where a thermocouple is also placed.

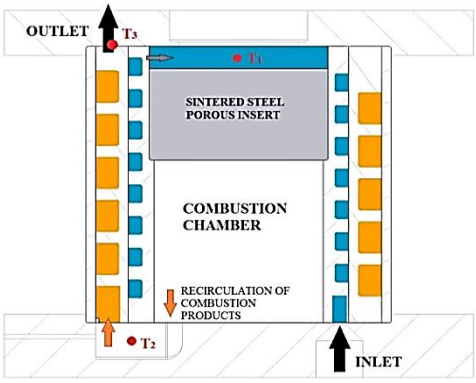

Figure 1. Section of the regenerative combustion chamber

The ignition of the mixture is obtained through a spark occurring in the gap between the porous flame holder and a stainless steel igniter inserted axially into the combustion chamber.

The combustor was designed with a diameter of 18 mm. This choice is imposed by the design point which was chosen to be at equivalence ratio (ϕ) of 0.65. This results in a laminar burning velocity of around 14 cm/s (according to the equation developed by Liao et al. [12]) which corresponds to a mass flow rate of 0.04 g/s. In a UMGT system assuming a turbine and compressor polytropic efficiency each of 0.7, the selected flow rate should produce 3 W of electrical output. As demonstrated in previous researches [13,14], increasing reactants' temperature and equivalence ratio also increases the burning velocity of the mixture, therefore the mass flow rate and the power output can be raised.

The cold fuel/air mixture enters the 1.5 mm helicoidal channel surrounding the cylindrical combustion and exits radially at the upper surface of the porous medium. After the combustion, the exhaust gases are recirculated through the outer helicoidal channel and exit axially. Combustion products are then collected (Figure 2 - right) and, after a condensation trap, sent to a Kane Auto5-1 gas analyser able to measure volumetric concentrations of unburned hydrocarbons (UHC), NO_x, CO_2, CO and O_2.

Figure 2. Combustion chamber with sintered steel porous insert (left) and rig setup (right)

Three K type thermocouples with wire diameter of 0.5 mm are placed at different locations in the combustion chamber, as shown in Figure 1, with the purpose of having a comprehensive understanding of the heat exchanges within the combustor's channels and of the grade of regeneration achieved. Specifically T_1 measures the preheating temperature of reactants before combustion, T_2 measures the temperature of the combustion products at the inlet of the exhaust channel and T_3 measures the temperature of the combustion products at the outlet. Also a B type thermocouple (Pt-Rh 30 %, Pt-Rh 6 %) with a 2 mm outer diameter ceramic sheath was used to measure the temperature in the combustion chamber at different axial positions. Flow rates are controlled using a Sierra SmartTrak 2 controller for air (with a minimum setpoint of 0.001 g/s of air and 1 % accuracy on the full range) and a Vögtlin Red-y controller for fuel (with an operating range between 100 ml/min to 6000 ml/min of air with accuracy of 1 % on the full scale). Since the fuel flow controller comes calibrated for utilization with air, a flow correction factor is used to accurately read the Liquefied Petroleum Gas (LPG) flow rate and the validation is made comparing the calculated equivalence ratio from the incoming flow rate with that calculated from the emission analysis.

Evaluated chemical formula	Density [kg/m^3]	Heating value [MJ/kg]	Specific heat [kJ/kg]	Stoichiometric fuel/air ratio
$C_{3.49}H_9$	2.28	46.048	1.653	0.0643

Table 1. Evaluated properties of LPG

As the fuel is an undefined mixture of mainly propane and butane, the flow rate calibration procedure also allows an evaluation of the fuel characteristics such as specific heat, density and subsequently its composition, heating value and combustion chemistry. A summary of the properties of LPG is shown in Table 1.

Results and discussion

As mentioned, several tests were run at different flow rates and equivalence ratios, mainly focusing on the lean side of combustion. The combustion chamber was started with a rich mixture and the equivalence ratio was progressively decreased with action on both flow controllers in order to maintain the total mass flow rate constant during the measurements. The equivalence ratio was decreased until the flame was able to sustain. Temperature readings were taken after the system reached steady conditions. These series of experiments were carried out on different days with an ambient temperature varying in the range 18-20 °C and a relative humidity between 38 and 55 %, therefore the influence of external conditions on heat transfer processes could be kept relatively constant.

Emissions analysis

The essential requirement for the combustion chamber is to achieve clean combustion. In Figure 3 the volume concentrations of CO_2, O_2 and CO are shown for a total mass flow rate of 0.04 g/s. As expected, the peak concentration of carbon dioxide is reached at equivalence ratio of 1 and at the same time oxygen concentration decreases to zero. Carbon monoxide in the exhaust gases appears when the mixture is slightly lean and increases considerably when it becomes rich. At stoichiometric conditions the volume percentage of CO is around 0.06 %. At higher flow rates the profiles are identical in shape and values to that in Figure 3, matching the combustion stoichiometry of LPG fuel.

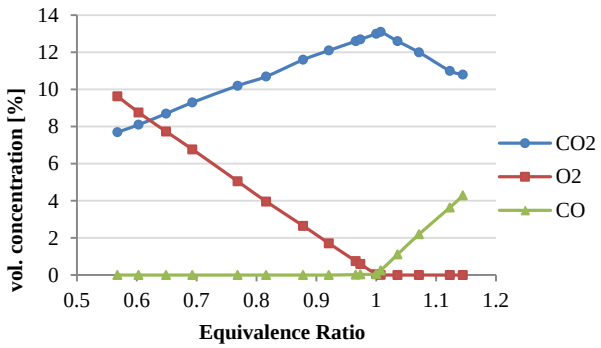

Figure 3. Volume concentration of main species in the combustion products at total mass flow rate of 0.04 g/s

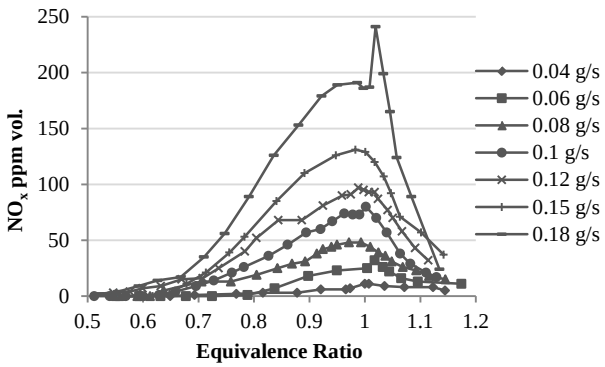

Figure 4. NO_x volume concentration in the combustion products at increasing mass flow rates

Volume concentrations of NO_x are also measured with the same analyser and the results are shown in Figure 4 for total flow rates ranging from 0.04 g/s to 0.18 g/s. The formation of NO_x is described by the Zeldovich mechanism and it depends on different factors, mainly high temperature, oxygen excess and fuel type and composition and this is confirmed by the present results, where the peak of concentration occurs at a slightly lean mixture ($\phi \approx 0.95$-0.98). Levels of unburned hydrocarbons were very low (between 0 and 2 ppm) at every flow rate and equivalence ratio considered. From the composition of the flue gases, the combustion efficiency was also computed employing the procedure of Stivender [15] for exhaust gases with the same background moisture (dry in this case), as given in Equation (1).

$$\eta_c = 1 - \left(\frac{\dot{m}_f + \dot{m}_{air}}{\dot{m}_f}\right)\left(\frac{\sum x_i M_i LHV_i}{LHV_f M_b}\right) \quad (1)$$

η_c represents the combustion efficiency, $\dot{m}_f$ and $\dot{m}_{air}$ are the fuel and air mass flow rates respectively, x_i is the mole fraction of the i^{th}-species (CO, UHC, H_2), M_i is the molecular weight of the i^{th}-species, LHV is the lower heating value and M_b is the molecular weight of the burned gases calculated as the weighted average of the species' molecular weights and their mole fraction in the combustion products. The plot of combustion efficiency at total mass flow rate of 0.04 g/s is shown in Figure 5. As it can be seen, the values of combustion efficiency on the lean side are always higher than 0.998, meaning an extremely clean combustion. As the equivalence ratio reaches stoichiometry, the efficiency slightly decreases to 0.997 and it becomes much lower when the fuel-air mixture gets richer.

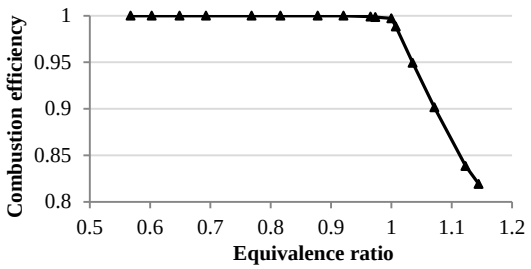

Figure 5. Combustion efficiency vs equivalence ratios at total mass flow rate of 0.04 g/s

Thermal characteristics

Temperatures were also monitored at different points in the combustion chamber, as described previously. Figure 6 and 7 show the temperature distribution in the inner cylinder along the centreline. Measurements were taken at six different distances from the porous insert: 1 mm, 2.5 mm, 5 mm, 7.5 mm, 10 mm and 12.5 mm. Equivalence ratios of 0.85 and 1 were considered and a correction was applied to the measured value as the thermocouple bead was directly exposed to the flame and radiation losses to the surrounding walls cannot be neglected. Equation (2) [16] was used for this correction and axial conduction was also taken into account.

$$T_g = T_b - \frac{\varepsilon_b \sigma (T_b^4 - T_w^4) + \left(k_b A_{cross} / L A_{surf}\right) \Delta T}{h} \quad (2)$$

T_g is the actual gas temperature, T_b is the measured temperature, ε_b and k_b are the emissivity and thermal conductivity of the bead respectively obtained from Hindasageri [17], T_w is the wall temperature, L is the wire length, A_{cross} and A_{surf} are the cross sectional area of the wire and the surface of the bead respectively, ΔT is the difference of temperature across the wire and h is the convection coefficient of the flow at the bead surface, obtained through Nu number [17].

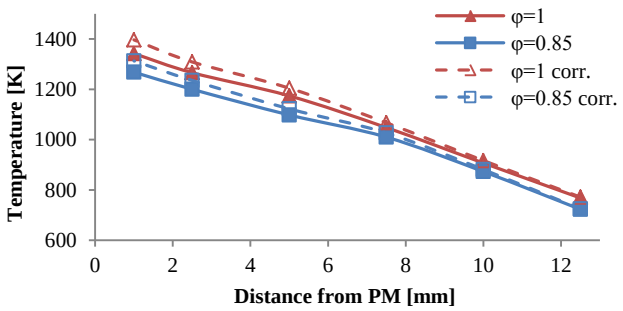

Figure 6. Temperature distribution at the centreline in the combustion chamber at total mass flow rate of 0.04 g/s

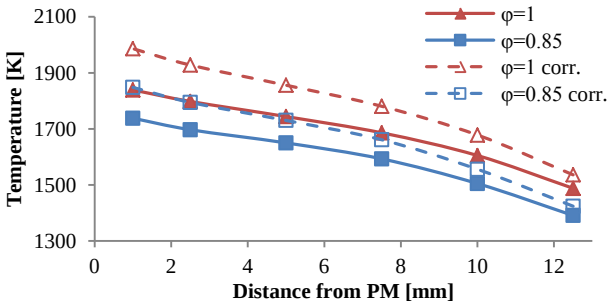

Figure 7. Temperature distribution at the centreline in the combustion chamber at total mass flow rate of 0.15 g/s

In Table 2 temperature values measured with the thermocouples T1, T2 and T3 are presented for equivalence ratios of 0.7 and 1 with total mass flow rates from 0.04 g/s to 0.18 g/s. As expected, the reactants temperature increases with the heat release rate in the combustion chamber. The auto ignition temperature of LPG is not well defined but it falls in the range 683 K – 853 K. In this case, when the total flow rate is higher than 0.1 g/s the preheating temperature reaches values of 708 K and 792 K and it keeps rising (up to 894 K for the cases considered) as the heat released is increased. The combustion chamber was designed in order to avoid autoignition and to prevent flashback in the channel where the "cold" reactants flow. In particular the hydraulic diameter of the channel was chosen to be lower than the quenching distance of the fuel. This also results in a flow velocity much higher than the laminar burning velocity so the flame would not be able to sustain in the channel and this is confirmed by the results obtained.

tot. flow rate	**ϕ = 0.7**			**ϕ = 1**		
	T1 [K]	*T2 [K]*	*T3 [K]*	*T1 [K]*	*T2 [K]*	*T3 [K]*
0.04 g/s	548	963	508	610	1032	555
0.06 g/s	623	1136	577	684	1201	623
0.08 g/s	655	1242	614	745	1325	684
0.1 g/s	708	1340	662	792	1447	729
0.12 g/s	726	1391	679	824	1529	763
0.15 g/s	732	-	685	842	-	780
0.18 g/s	800	-	759	894	-	840

Table 2. Values of temperature T1, T2 and T3 at equivalence ratio of 0.7 and 1

At 0.15 g/s and 0.18 g/s temperature T2 became too high for the type of thermocouple used in the recirculation cavity and the output values were extremely inaccurate. Temperature measurements also allowed the evaluation of the amount of heat transferred to the cold mixture from the combustion products. Heat rates were calculated using the inlet temperature and the final preheating temperature of the reactants and then related to the heat released from the combustion.

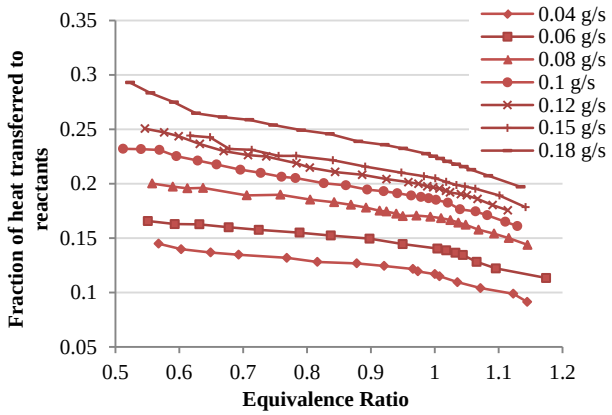

Figure 8. Fraction of the heat released from combustion transferred to the reactants at varying equivalence ratios and total flow rates

These values of temperature are somewhat close to the ones presented by Turkeli-Ramadan [18] on a similar regenerative combustion chamber with a smaller diameter. The plots in Figure 8 show how the heat transferred to the reactants changes at different equivalence ratios and flow rates. It is interesting to note that at low equivalence ratios, thus lower HRR, the heat fraction results increased compared to higher equivalence ratios. Generally the level of regeneration obtained is good, as 13% to 30% of the heat contained in the combustion products in the cases considered can be used to preheat the reactants. Increasing the flow rate, thus the heat released, is expected to further raise this percentage.

Conclusions

In order to develop a complete UMGT system, this study proposes a regenerative combustion chamber operating with premixed combustion of LPG. The main purpose of the combustor is to recover the heat contained in the combustion products to increase the temperature of the reactants, with obvious benefits in terms of thermal efficiency. Excellent results were obtained in terms of pollutant emissions, achieving over 99.6% of combustion efficiency for lean mixtures at all the mass flow rates considered. Good grade of regeneration was also achieved as an amount of heat ranging from 13% to 30% of the heat released from the combustion was transferred to the cold reactants.

Acknowledgments

The authors would like to thank Alan Eaton and Martin Ryder whose contribution for the successful setup of test rig was essential. The authors are also thankful for the support received from the Energy and Fuels Research Unit (EFRU) of the University of Auckland for this research in the academic years 2015 and 2016.

References

[1] Z. Turkeli-Ramadan, R. Sharma, R. Raine, Clean flat flame combustor for ultra micro gas turbine, Proceedings of the 19th Australasian Fluid Mechanics Conference (2014).

[2] T. Sakurai, S. Yuasa, T. Honda, Concept and Experiment of a Propane-fueled Flat-Flame Ultra-Micro Combustor for UMGT, Proceedings of the International Gas Turbine Congress (2007).

[3] A. Epstein, Millimeter-Scale, Micro-Electro- Mechanical Systems Gas Turbine Engines, Journal of Engineering for Gas Turbines and Power. 126 (April 2004).

[4] R. Capata, E. Sciubba, Preliminary considerations on the thermodynamic feasibility and possible design of ultra-, micro- and nano-gas turbines, International Journal of Thermodynamics. 9 (2006) 81-91.

[5] R. Capata, Ultra Micro Gas Turbines, Efficiency, Performance and Robustness of Gas Turbines, (2012).

[6] A. Diango, C. Périlhon, E. Danho, G. Descombes, Influence of Heat Transfer on Gas Turbine Performance, InTech. Advances in Gas Turbine Technology (2011).

[7] D. Reynaerts, J. Van Den Braembussche, P. Hendrick, M. Baelmans, J. Driesen, R. Puers, F. Al-Bender, J. Peirs, T. Waumans, P. Vleugels, K. Liu, K. Alsalihi, A. Di Sante, T. Verstraete, D. Verstraete, J. Trilla, T. Stevens, F. Rogiers, S. Stevens, F. Ceyssens, Development of a gas turbine with a 20 mm rotor: review and perspectives, The Sixth International Workshop on Micro and Nanotechnology for Power Generation and Energy Conversion Applications (2006).

[8] J. Peirs, D. Reynaerts, F. Verplaetsen, Development of an axial microturbine for a portable gas turbine generator, J Micromech Microengineering. 13 (2003) S190.

[9] O. Dessornes, S. Landais, R. Valle, A. Fourmaux, S. Burguburu, C. Zwyssig, Z. Kozanecki, Advances in the Development of a Microturbine Engine, Journal of Engineering for Gas Turbines and Power. 136 (July 2014).

[10] jqrmag.com, A promising technology for powering humanoid robots? – Development of an Ultra-compact Gas Turbine Capable of Generating Large Amounts of Power Anywhere, (May, 2012).

[11] Z. Turkeli-Ramadan, R. Sharma, R. Raine, Experimental investigation of the effects of preheating on the flame stability of natural gas-air premixture of a flat flame micro combustor for ultra micro gas turbine, ISABE-2013-1705. (2013).

[12] S.Y. Liao, D.M. Jiang, Q. Cheng, Determination of laminar burning velocities for natural gas, Fuel. 83 (2004) 1247-1250.

[13] Z. Turkeli-Ramadan, R.N. Sharma, R.R. Raine, Two-dimensional simulation of premixed laminar flame at microscale, Chem. Eng. Sci. 138 (2015) 414-431.

[14] V. Giovannoni, R.N. Sharma, R.R. Raine, Premixed combustion of methane–air mixture stabilized over porous medium: A 2D numerical study, Chemical Engineering Science. 152 (2016) 591-605.

[15] D. Stivender, Development of a Fuel-Based Mass Emission Measurement Procedure, SAE (1971).

[16] S. Krishnan, B.M. Kumfer, W. Wu, J. Li, A. Nehorai, R.L. Axelbaum, An Approach to Thermocouple Measurements That Reduces Uncertainties in High-Temperature Environments, - Energy Fuels. (2015) - 3446.

[17] V. Hindasageri, R.P. Vedula, S.V. Prabhu, Thermocouple error correction for measuring the flame temperature with determination of emissivity and heat transfer coefficient, Rev. Sci. Instrum. 84 (2013) 024902.

[18] Z. Turkeli-Ramadan, R. Sharma, K. Yamaguchi, Combustion characteristics of HEX-Combustor for Ultra Micro Gas Turbine, (2011).